ФИЗИКА ЭЛЕМЕНТАРНЫХ ЧАСТИЦ И АТОМНОГО ЯДРА
2014. Т. 45. ВЫП. 4

SCATTERING AMPLITUDES OF QCD STRING IN THE WORLDLINE FORMALISM

Yu. Makeenko[*]

Institute of Theoretical and Experimental Physics, Moscow

[*]E-mail: makeenko@itep.ru

ФИЗИКА ЭЛЕМЕНТАРНЫХ ЧАСТИЦ И АТОМНОГО ЯДРА
2014. Т. 45. ВЫП. 4

SCATTERING AMPLITUDES OF QCD STRING IN THE WORLDLINE FORMALISM

Yu. Makeenko[*]

Institute of Theoretical and Experimental Physics, Moscow

The derivation of large-N QCD meson-scattering amplitudes in the Regge regime, where the effective theory of long strings is applied in $d = 4$, is reviewed. A special attention is paid to the reparameterization path integral which plays a crucial role in the consistency of off-shell amplitudes. I show how the linear Reggeon trajectory is obtained for QCD string in the mean-field approximation, which turns out to be exact for the Nambu–Goto string, and discuss the interrelation with perturbative QCD.

Дан обзор вывода амплитуд рассеяния мезонов для струны КХД при больших N в режиме Редже, когда в $d = 4$ применима эффективная теория длинных струн. Особое внимание уделено континуальному интегралу по репараметризациям, который играет ключевую роль для самосогласованности амплитуд вне массовой поверхности. Показано, как линейная траектория Редже возникает для струны КХД в приближении среднего поля, которое является точным для струны Намбу–Гото, а также обсуждается взаимосвязь с пертурбативной КХД.

PACS: 12.40.Nn

INTRODUCTION

QCD string is made from fluxes of the gluon field and makes sense for the distances larger than the confinement scale. There are two cases where QCD string is described by an effective theory of long strings: the static potential (reviewed in [1]) and meson scattering amplitudes in the Regge regime described in this talk. I review the results of [2–9], where the scattering amplitudes of QCD string were obtained in the Regge regime, using the worldline formalism.

For the consistency of the (off-shell) amplitudes, a very important role is played by the reparameterization path integral (a synonym of the path integral over boundary metrics or the path integral over boundary values of the Liouville field). This issue is reviewed in Sec. 1 of this talk.

Sections 2 and 3 are devoted to scattering amplitudes of fundamental string and QCD string in the Regge regime. I consider (polygonal) momentum Wilson

[*]E-mail: makeenko@itep.ru

loops, semiclassical fluctuations about the associated minimal surface and the mean-field approach to the Reggeon trajectory in $d = 4$. I also discuss off-shell scattering amplitudes of fundamental string and the relative contribution of perturbative QCD to QCD string.

1. REPARAMETERIZATION PATH INTEGRAL

1.1. Path Integral over Reparameterizations. It is commonly believed that the Wilson loop of large size in large-N QCD equals the string disk amplitude. As was emphasized by Polyakov [10], it is important to path-integrate over reparameterizations of the boundary:

$$W[x(\cdot)] = \int \mathcal{D}_{\rm diff} t(s)\, \mathrm{e}^{-KS[x(t)]}\,, \tag{1}$$

i.e., over functions $t(s)$ with $\dot{t}(s) \equiv dt(s)/ds \geqslant 0$ (here $K = 1/2\pi\alpha'$ is the string tension).

The necessity for reparameterizations of the boundary curve within the Polyakov string formulation was pointed out long ago by Polyakov [11] and Alvarez [12]. The path integral over reparameterizations first appeared for an off-shell propagator in [13].

The boundary action $S[x(t)]$ in Eq. (1) reads explicitly

$$S[x(t)] = \frac{1}{4\pi} \int\limits_{-\infty}^{+\infty} \frac{ds_1 ds_2}{(s_1 - s_2)^2} \left[x(t(s_1)) - x(t(s_2))\right]^2 \tag{2}$$

for the upper half-plane parameterization of the string worldsheet, where the boundary is parameterized by the real axis. It is known from Douglas [14] algorithm of solving the Plateau problem (finding the minimal surface), which prescribes to minimize the boundary functional (2) with respect to reparameterizations $t(s)$. The boundary curve in Eq. (2) is fixed, so the boundary action is a functional of $t(s)$.

A few comments are in order:

• The representation (1) can be derived for the Polyakov string in critical dimension $d = 26$ by doing the Gaussian path integral over string worldsheets with fixed boundary. The Liouville field φ, which enters through the conformal factor of the 2D metric tensor $g_{ab} = \mathrm{e}^{\varphi}\delta_{ab}$, decouples then in the bulk, while its boundary value is related to the reparameterizations as

$$\frac{dt(s)}{ds} = \mathrm{e}^{\varphi(s,0)/2}. \tag{3}$$

Thus, the path integral over reparameterizations is the same as that over boundary metrics.

• For the function $t(s) = t_*(s)$, minimizing Douglas' integral (2), the embedding-space coordinates obey the conformal gauge (*i.e.*, the Virasoro constraints), so the quadratic stringy action coincides with the Nambu–Goto action. This is why the boundary action (2) reproduces the minimal area.

• The area law for asymptotically large loops can be obtained as a saddle point in the reparameterization path integral (1) at $t(s) = t_*(s)$. It can be shown that the zig-zag (or backtracking) symmetry holds, as it should for the minimal area, owing to an explicit form of $t_*(s)$.

• The coordinates $x^\mu(t)$ enter the boundary action (2) quadratically, which makes it easy to further integrate over the boundary curves. The nonlinearities of the problem then reside in the reparameterization path integral.

• In $d < 26$, the ansatz (1) has to be modified by incorporating the path integral over bulk fields, as is given by the effective string theory of Polchinski, Strominger [15] reviewed in [1]. The reparameterization path integral remains crucial for the consistency.

Integrating by parts, Douglas' integral can be rewritten as

$$S[x(t(s))] = \frac{1}{2}\int\limits_{-\infty}^{+\infty} dt_1 dt_2\, \dot{x}(t_1)\cdot\dot{x}(t_2)\, G\left(s(t_1)-s(t_2)\right),$$
$$G\left(s_1-s_2\right) = -\frac{1}{\pi}\ln|s_1-s_2|, \tag{4}$$

and the reparameterization path integral goes over the inverse functions $s(t)$.

1.2. Nontrivial Example: Ellipse. A simple nontrivial example, showing the need of the boundary reparameterization, is an elliptic boundary curve. Using the unit-disk parameterization $z = r\,\mathrm{e}^{\mathrm{i}\phi}$, we write it as

$$x^1 = a\cos\theta(\phi), \qquad x^2 = b\sin\theta(\phi), \tag{5}$$

where a and b are the major and minor radii of the ellipse and $\theta(\phi)$ with $\dot{\theta}(\phi) \geqslant 0$ reparameterizes the boundary.

Suppose $\theta_*(\phi) = \phi$, then Douglas' integral equals

$$S[x(\theta)] = \pi\frac{a^2+b^2}{2} \quad \text{rather than} \quad \pi ab. \tag{6}$$

The equality is only for a circle $a = b$, when the unit-disk coordinates are conformal (or isothermal).

The minimization of Douglas' integral (2) for an ellipse gives for $\theta(\phi)$ the incomplete elliptic integral:

$$\dot{\theta}_*(\phi) = \frac{\pi}{2K(\nu)} \frac{1}{\sqrt{(1-\nu)^2 + 4\nu \sin^2 \phi}}, \qquad \frac{\pi K\left(\sqrt{1-\nu^2}\right)}{2K\left(\nu\right)} = \log \frac{a+b}{a-b}, \quad (7)$$

where $K(\nu)$ is the complete elliptic integral of the first kind. These formulas can be obtained by conformal mapping of a unit disk onto the interior of an ellipse.

We explicitly see from this simple example how the reparameterization of the boundary is needed to recover the minimal area.

1.3. Large Loops and Minimal Area. The area law (= the exponential of (minus) the minimal area) is thus recovered from the reparameterization path integral (1) in the saddle-point approximation.

Gaussian fluctuations about the saddle-point $t_*(s)$ result in a pre-exponential factor:

$$W\left[x(\cdot)\right] \overset{\text{large loops}}{=} F\left[\sqrt{K}x(\cdot)\right] \, \mathrm{e}^{-KS_{\min}[x(\cdot)]} \left[1 + \mathcal{O}\left((KS_{\min})^{-1}\right)\right], \quad (8)$$

which is contour-dependent. Its contribution for large loops is much less than that of the minimal area.

This pre-exponential factor shows up, however, in more subtle effects (such as the Lüscher term), coming from fluctuations about $t_*(s)$:

$$t(s) = t_*(s) + \frac{\beta(s)}{\sqrt{KS_{\min}}}. \quad (9)$$

For a $R \times T$ rectangle with $TR \gg 1/K$ and $T \gg R$, it is possible to path-integrate over $\beta(s)$, as is done in [6], to obtain

$$F\left(\text{rectangle}\right) \propto \mathrm{e}^{\pi T/R} \qquad \text{for } T \gg R \quad (10)$$

reproducing the Lüscher term for bosonic string in $d = 26$. To this order we can restrict ourselves with the quadratic approximation in $\beta(s)$, so it is not essential what is the actual measure in Eq. (1).

This demonstrates that the reparameterization path integral (1) knows about the bulk fluctuations.

1.4. Discretization of the Measure. To construct the measure on $\mathrm{Diff}\left(\mathbb{R}\right)$ in Eq. (1), we split the interval $[s_0, s_f]$ into N pieces and define [3]

$$\int\limits_{\substack{s(\tau_0)=s_0 \\ s(\tau_f)=s_f}} \mathcal{D}_{\text{diff}} s(\tau) \cdots = \lim_{N\to\infty} \int\limits_{s_0}^{s_f} \prod_{j=1}^{N-1} \int\limits_{s_0}^{s_{j+1}} ds_j \, \frac{1}{(s_{j+1} - s_j)} \frac{1}{(s_1 - s_0)} \cdots, \quad (11)$$

where the integration goes over $(N-1)$ subordinated values $s_1, \ldots, s_{N-1}$: $s_0 \leqslant \ldots \leqslant s_{i-1} \leqslant s_i \leqslant \ldots \leqslant s_N = s_f$. Thus defined measure is covariant under reparameterizations

$$s \to t(s), \quad t(s_0) = s_0, \quad t(s_f) = s_f, \quad \frac{dt}{ds} \geqslant 0. \tag{12}$$

Discretizing $s' = \exp[-\varphi]$ that relates reparameterizations to the boundary value of the Liouville field φ by $s_i - s_{i-1} = \exp[-\varphi_i]$, we write the measure (11) as

$$\int\limits_{s_0}^{s_f} \mathcal{D}_{\text{diff}} s \ldots = \lim_{N\to\infty} \prod_{i=1}^{N} \int\limits_{-\infty}^{+\infty} d\varphi_i \, \delta^{(1)}\Big(s_f - s_0 - \sum_{j=1}^{N} \mathrm{e}^{-\varphi_j}\Big) \ldots \tag{13}$$

with the only restriction on φ_i's given by the delta function.

The integral over s_i in Eq. (11) is (logarithmically) divergent and can be nicely regularized by changing

$$\frac{1}{(s_i - s_{i-1})} \longrightarrow \frac{1}{\Gamma(\delta_i)(s_i - s_{i-1})^{1-\delta_i}}, \qquad \text{all} \quad \delta_i = \delta. \tag{14}$$

The main integral for the integration at the intermediate point s_i is

$$\int\limits_{s_{i-1}}^{s_{i+1}} ds_i \, \frac{\Gamma^{-1}(\delta_i)\Gamma^{-1}(\delta_{i+1})}{(s_{i+1} - s_i)^{1-\delta_{i+1}}(s_i - s_{i-1})^{1-\delta_i}} = \frac{\Gamma^{-1}(\delta_i + \delta_{i+1})}{(s_{i+1} - s_{i-1})^{1-\delta_i-\delta_{i+1}}} \, . \tag{15}$$

This is an analogue of the well-known convolution formula

$$\int\limits_{-\infty}^{+\infty} \frac{ds_i}{\sqrt{2\pi}} \frac{\mathrm{e}^{-(s_f - s_i)^2/2\nu_1}}{\sqrt{\nu_1}} \frac{\mathrm{e}^{-(s_i - s_0)^2/2\nu_2}}{\sqrt{\nu_2}} = \frac{\mathrm{e}^{-(s_f - s_0)^2/2(\nu_1+\nu_2)}}{\sqrt{(\nu_1 + \nu_2)}} \tag{16}$$

used for calculations of Feynman's path integral with the usual Wiener measure.

The functional limit is reached when $N \to \infty$ with $N\delta \to 0$:

$$\int\limits_{s_0}^{s_N = s_f} \mathcal{D}^{(N)}_{\text{diff}} s = \frac{1}{\Gamma(N\delta)} \frac{1}{(s_N - s_0)^{1-N\delta}} \overset{N\delta\to 0}{\longrightarrow} N\delta \frac{1}{(s_f - s_0)} \, , \tag{17}$$

reproducing the projective-covariant result. This is an analogue of the free propagator.

1.5. Reparameterizations as Lévy Stochastic Process. What trajectories are typical in the path integral over reparameterizations?

To answer this question, Buividivich and Makeenko [4] consider a subordinated stochastic process (called the gamma-subordinator) with the probability density function

$$P\left(\Delta s_i\right) = \frac{1}{\Gamma(\delta)\left(\Delta s_i\right)^{1-\delta}}, \tag{18}$$

with $\delta > 0$ being a time step. Then

$$ds_f \int\limits_{s_0}^{s_f} \mathcal{D}_{\text{diff}}^{(N)} s \tag{19}$$

has the meaning of a propagator from s_0 to $[s_f, s_f + ds_f]$ during the time $\tau = N\delta$.

Introducing the scaling variable

$$z = \tau \ln \frac{1}{\left(s_f - s_0\right)}, \tag{20}$$

which is analogous to $(s_f - s_0)^2/\tau$ for the Gaussian random walks, we write

$$\frac{\tau\, ds_f}{\left(s_f - s_0\right)^{1-\tau}} = dz\, \mathrm{e}^{-z}. \tag{21}$$

Therefore, a scaling occurs with

$$\left(s_f - s_0\right) \sim \mathrm{e}^{-1/\tau}, \tag{22}$$

and we conclude that the Hausdorff dimension $d_H = 0$ in this case. This supersedes $(s_f - s_0)^2 \sim \tau$ for the Gaussian stochastic process of the Brownian motion (whose $d_H = 2$).

Typical trajectories for the gamma-subordinator can be obtained by the Metropolis–Hastings algorithm in spite of several subtleties, such as the central limit theorem and/or the law of large numbers are not applicable for the probability density (18) which has an infinite dispersion. The results are depicted in Fig. 1, *a* and *b* for $\delta = 0.5$ and $\delta = 0.09$, respectively. Lévy's flights are seen in plot *b*. Their origin is that $P(\Delta s_i)$ is very large at small $\Delta s_i \Longrightarrow$ most of Δs_i's are small. Then some of Δs_i has to be large to satisfy the boundary condition.

1.6. Hausdorff Dimension of Sample Trajectories. The Hausdorff dimension of the gamma-subordinator is expected to decrease from 1 to 0 with decreasing δ, as discussed by Horowitz [16].

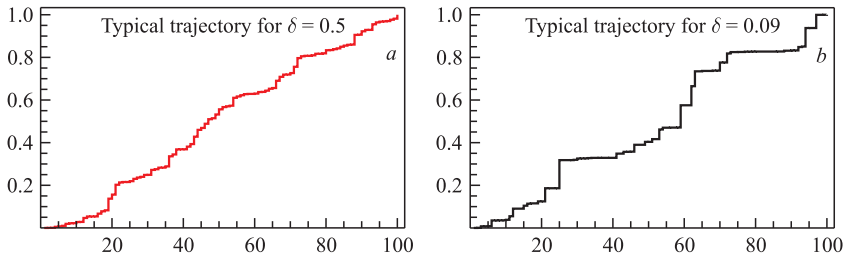

Fig. 1. Typical trajectories for the gamma-subordinator obtained by the Metropolis–Hastings algorithm. Lévy's flights are seen in plot *b*

The Hausdorff dimension of the discretized process is determined by its (Lévy–Khintchine) characteristic function as

$$d_H = \lim_{q\to\infty} \frac{\ln\left(-N \ln\left\langle \mathrm{e}^{-q\Delta s_i}\right\rangle\right)}{\ln q}. \tag{23}$$

This definition is equivalent to a more familiar one based on the covering by balls.

For the probability density (18), Buividovich and Makeenko [4] found

$$\left\langle \mathrm{e}^{-q\Delta s_i}\right\rangle = {}_1F_1(\delta, \delta N; -q), \tag{24}$$

where ${}_1F_1$ is the confluent hypergeometric function. Substituting in Eq. (23), we obtain the Hausdorff dimension plotted versus $\ln(1/\delta)$ in Fig. 2, *a*. The values of d_H are extracted from the slope of the lines in Fig. 2, *b*. The Hausdorff dimension decreases from 1 for $\delta \gtrsim 1$ to 0 for $\delta N \to 0$, thus confirming the consideration of Horowitz [16].

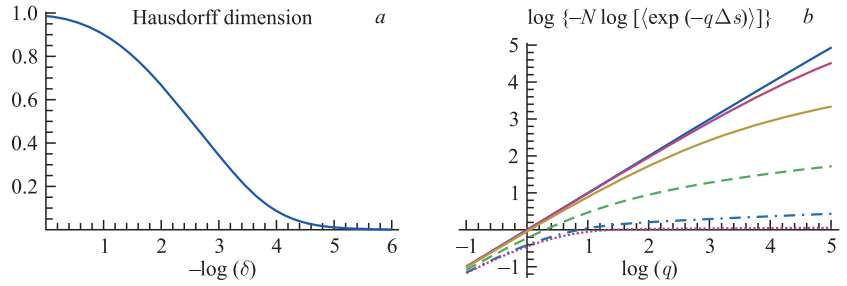

Fig. 2. Hausdorff dimension versus $\ln(1/\delta)$ (*a*) extracted from the slope of the lines in plot *b* for $\delta = 1,\ 10^{-1},\ 10^{-2},\ 10^{-3},\ 10^{-4},\ 10^{-5}$ from the top to the bottom

1.7. Ambiguities of the Measure. The discretization of the measure displayed on the right-hand side of Eq. (11) is not unique. A more symmetric discretization of the measure reads

$$\mathcal{D}_{\rm diff}s = \prod_{i=1}^{N-1} ds_i \frac{(s_{i+1}-s_{i-1})}{(s_{i+1}-s_i)(s_i-s_{i-1})} \quad \text{Lovelace choice.} \tag{25}$$

Every multiplier is now invariant under the $PSL(2;\mathbb{R})$ projective transformations

$$s \Rightarrow \frac{as+b}{cs+d} \qquad \text{with} \quad ad-bc=1, \tag{26}$$

which form a subgroup of the reparameterizations. For the measure (11) only the product over j was invariant under $PSL(2;\mathbb{R})$.

The measure (25) was considered in some detail in [6], and results in consistent off-shell (Lovelace) string amplitudes of the intercept $\alpha(0)=(d-2)/24$ are described below in Subsec. 3.1.

It is worth noting that the results do not change if the next-to-neighbor points are involved in the discretization, *i.e.*,

$$(s_{i+1}-s_i) \Longrightarrow (s_{i+n}-s_i)/n\,. \tag{27}$$

This supports the expectation that a continuum limit exists in spite of the discontinuities of the trajectories. However, the measures (11) and (25) apparently belong to different universality classes (which differ by the value of $\alpha(0)$).

2. SCATTERING AMPLITUDES AS MOMENTUM LOOPS

2.1. Momentum Loops. As was first pointed out by Migdal [17], scattering amplitudes are given by the reparameterization-invariant functional Fourier transformation

$$A[p(\cdot)] = \int \mathcal{D}x \, \exp\left(\mathrm{i}\int p\cdot dx\right) J[x(\cdot)]\, W[x(\cdot)], \qquad \text{with process-dependent} \quad J[x(\cdot)] \tag{28}$$

of the Wilson loop (to be identified with the string disk amplitude) for a piecewise constant momentum loop

$$p^\mu(t) = P_i^\mu \qquad \text{for} \quad t_i < t < t_{i+1}, \tag{29}$$

which is schematically depicted in Fig. 3.

Differentiating the step function, we obtain

$$\dot{p}^\mu(t) = -\sum_i p_i^\mu \delta(t-t_i), \tag{30}$$

Fig. 3. Piecewise constant momentum loop

with $p_i^\mu \equiv P_{i-1}^\mu - P_i^\mu$ representing M momenta of (all incoming) particles. Then momentum conservation is automatic while an (infinite) volume V is produced, say, by integration over $x_0 = x_M$.

The Fourier transformation of the string vertex operators can be reproduced as follows. For scalars we simply integrate by parts

$$\int dt\, p(t)\cdot\dot{x}(t) = -\int dt\, \dot{p}(t)\cdot x(t) = \sum_i p_i\cdot x_i\,. \tag{31}$$

For vectors we first apply the variational derivative $\delta/\delta p^\mu(t)$ for an arbitrary $p^\mu(t)$, which inserts $\mathrm{i}\dot{x}^\mu(t)$, and then set $p^\mu(t)$ to be piecewise constant. It is similar for higher spins.

2.2. Momentum Disk Amplitude. After the Gaussian path integration over $\mathcal{D}x^\mu(t)$ (which produces an s-independent determinant) we get the amplitude

$$A[p(\cdot)] = \int \mathcal{D}_{\mathrm{diff}} s(t) \exp\left(\alpha' \int\limits_{-\infty}^{+\infty} dt_1 \int\limits_{-\infty}^{+\infty} dt_2\, \dot{p}(t_1)\cdot\dot{p}(t_2)\, \ln|s(t_1)-s(t_2)|\right), \tag{32}$$

which looks like the disk amplitude (1) (the Wilson loop) for the boundary curve

$$x^\mu(t) = \frac{1}{K} p^\mu(t). \tag{33}$$

This can be seen by comparing the exponent in Eq. (32) with (4).

Actually, the discontinuities of the stepwise momentum loop are always smeared by a regularization which involves the boundary Liouville field $\varphi_i = \varphi(s_i, 0)$ for the covariance as will be momentarily discussed:

$$p^\mu(t) = \frac{1}{\pi}\sum_i p_i^\mu \arctan\frac{(t-t_i)}{\varepsilon_i} \overset{\varepsilon_i\to 0}{\longrightarrow} \frac{1}{2}\sum_i p_i^\mu \operatorname{sign}(t-t_i), \qquad \varepsilon_i = \varepsilon\, \mathrm{e}^{-\varphi_i}. \tag{34}$$

An embedding space image of thus smeared stepwise function is a polygon with vertices

$$x_i^\mu = \frac{1}{K} P_i^\mu, \qquad x_i^\mu - x_{i-1}^\mu = \frac{1}{K} p_i^\mu, \tag{35}$$

as is depicted in Fig. 4. This looks similar to the Wilson-loop/scattering-amplitude duality for $\mathcal{N} = 4$ SYM advocated by Alday, Maldacena [18], Drummond, Korchemsky, Sokatchev [19], Brandhuber, Heslop, Travaglini [20].

Fig. 4. Stepwise momentum loop (top left) smeared with the width ε_i (bottom left) and its polygonal image in embedding space (right)

2.3. Invariant Regularization and the Liouville Field. The invariant regularization used in the previous subsection plays a very important role for the consistency of scattering amplitudes. For smeared stepwise $p^\mu(t)$ the Gaussian exponent reads

$$-\pi \int_{-\infty}^{+\infty} dt_1\, dt_2\, \dot{p}(t_1)\cdot\dot{p}(t_2)\, G\left(s(t_1), s(t_2)\right) = \\ = \sum_{k\neq l} p_k\cdot p_l \log|s_k - s_l| - \pi \sum_j p_j^2 G(s_j, s_j). \quad (36)$$

The Green function $G(s_i, s_j)$ has to be regularized at coinciding arguments, say, for $|s_i - s_j| \lesssim \varepsilon_i, \varepsilon_j$, which must be done compatible with the boundary metric for the regularization to be invariant. Therefore $G(s_j, s_j)$ has to involve the Liouville field φ ($g_{ab} = \mathrm{e}^{\varphi}\delta_{ab}$) as pointed out by Polyakov [11]:

$$G(s_i, s_j) = -\frac{1}{\pi}\ln|s_i - s_j| \qquad \text{for } |s_i - s_j| \gg \varepsilon_i, \varepsilon_j, \\ G(s_j, s_j) \longrightarrow G_\varepsilon(s_j, s_j) = \frac{1}{\pi}\log\frac{1}{\varepsilon} + \frac{1}{2\pi}\varphi(s_j, 0). \quad (37)$$

For critical open bosonic string (in $d = 26$) Aoyama, Dhar, Namazie [21] wrote explicitly

$$A\left(p_1, \ldots, p_M\right) = \\ = \int \mathcal{D}\varphi(s) \int \prod_m ds_m\, \mathrm{e}^{\varphi(s_m,0)/2 - \pi\alpha' p_m^2 G(s_m, s_m)} \prod_{j\neq m} |s_j - s_m|^{\alpha' p_j\cdot p_m}, \quad (38)$$

where the integration over s_m also involves the boundary metric $\mathrm{e}^{\varphi/2}$. In view of Eq. (37), the path integration over $\varphi(s, 0)$ — the boundary value of the Liouville field — decouples, but only on shell, *i.e.*, for tachyonic scalar, massless vector,

etc. For off-shell amplitudes it has to be properly taken into account as is described in this paper.

2.4. Classical (Long-String) Limit. At the classical level we are interested in the saddle-point approximation to Eq. (32). The minimal surface spanned by a rectangle with stepwise $p^\mu(t)$ displayed in Eq. (34) is given by the harmonic function

$$X^\mu(x,y) = \frac{1}{\pi K}\sum_i p_i^\mu \arctan\frac{(x-s_i)}{y}, \qquad s_i = s(t_i), \tag{39}$$

as found in [7]. It is T-dual to a more familiar (pure imaginary) one

$$X^\mu(x,y) = \frac{\mathrm{i}}{2\pi K}\sum_i p_i^\mu \ln\left[(x-s_i)^2+y^2\right], \qquad s_i = s(t_i) \tag{40}$$

in coordinate space, known from the early days of string theory [22].

Douglas' minimization with respect to s_i's results (for $p_i\cdot p_j \gg p_i^2, p_j^2$) in the set of equations

$$\sum_{j\neq i}\frac{p_i\cdot p_j}{s_i-s_j} = 0. \tag{41}$$

Only $M-3$ of these are independent because of the $PSL(2;\mathbb{R})$ projective invariance.

For $M=4$, we set $s_1=0$, $s_3=1$, $s_4=\infty$ in the usual way and obtain

$$s_{2\,*} = \frac{s}{s+t}. \tag{42}$$

Otherwise the projective-invariant ratio is fixed to be

$$\left(\frac{s_{21}s_{43}}{s_{31}s_{42}}\right)_* = \frac{s}{s+t}. \tag{43}$$

This value is well known from the saddle point of the Veneziano amplitude at large $-s,-t$.

The polygon bounds the minimal surface of the area

$$KS_{\min} = \alpha' s\ln\frac{s}{s+t} + \alpha' t\ln\frac{t}{s+t} \overset{-s\gg -t}{\to} -\alpha' t\ln\frac{s}{t}, \tag{44}$$

whose exponential reproduces the classical Regge behavior:

$$A(s,t) = \mathrm{e}^{-KS_{\min}} \propto s^{\alpha' t}. \tag{45}$$

2.5. Momentum Lüscher Term. It is easy to account for semiclassical fluctuations about the minimal surface. To make a connection with the usual computation of the Lüscher term for a $T \times R$ rectangle, we perform the Schwarz–Christoffel map of the upper half-plane onto the rectangle:

$$\omega(z) = \sqrt{s_{42}s_{31}} \int_{s_2}^{z} \frac{dx}{\sqrt{(s_4 - x)(s_3 - x)(x - s_2)(x - s_1)}}, \tag{46}$$

with

$$R = 2K\left(\sqrt{1-r}\right) \overset{r\to 1}{\to} \pi, \qquad T = 2K\left(\sqrt{r}\right) \overset{r\to 1}{\to} \ln\frac{16}{1-r}, \tag{47}$$

where

$$r \equiv \frac{s_{43}s_{21}}{s_{42}s_{31}} = \frac{s}{s+t}, \qquad s_{ij} = s_i - s_j, \tag{48}$$

is the projective-invariant ratio. Therefore, the ratio

$$\frac{T}{R} = \frac{K\left(\sqrt{r}\right)}{K\left(\sqrt{1-r}\right)} \overset{r\to 1}{\to} \frac{1}{24\pi} \ln\frac{16s}{t} \tag{49}$$

is also projective invariant.

Like for the static potential, each degree of freedom results in the momentum-space Lüscher term computed by Janik [23], Y. M. [7]

$$\frac{\pi T}{24R} = \frac{1}{24} \ln\frac{16s}{t}, \tag{50}$$

where in the Regge regime we have used the asymptote (49).

2.6. Semiclassical Reggeon Intercept. There are $(d-2)$ such sets of degrees of freedom for bosonic string, so we obtain the linear Regge trajectory

$$\alpha(t) = \frac{d-2}{24} + \alpha' t. \tag{51}$$

Here $\alpha' t$ comes from the classical amplitude (45), while the intercept comes from exponentiating the momentum Lüscher term on the right-hand side of Eq. (50).

In the effective string theory description of QCD string, the parameter

$$\ln\frac{1}{1-r} = \ln\frac{s}{t} \tag{52}$$

plays for scattering amplitudes the role of T for the static potential. The Regge behavior is like the area law:

$$A \propto \mathrm{e}^{\alpha(t)\ln(s/t)} \quad \text{is similar to} \quad W \propto \mathrm{e}^{-TV(R)}, \tag{53}$$

while the expansion of $\alpha(t)$ in $(-1/t)$ is like the expansion of $V(R)$ in $1/R$. This is one more manifestation of the Wilson-loop/scattering-amplitude duality.

The semiclassical correction to the Regge trajectory of the effective string theory in $d < 26$ can be alternatively computed for the upper-half plane parameterization, repeating that of Durhuus, Olesen, Petersen [24] for the static potential of the Polyakov string. Now the same result emerges as

$$\alpha(0) = 1 + \frac{d-26}{24} = \frac{d-2}{24}, \tag{54}$$

where 1 comes from the boundary Liouville field and $(d-26)/24$ comes from the bulk fluctuations of the effective string.

We thus see the important difference in how the Lüscher term emerges for the worldsheet and upper-half plane parameterizations: for the former it is due to quantum fluctuations of $X^\mu(\tau,\sigma)$, while for the latter it comes entirely from the classical part of the Liouville field (= the induced metric).

2.7. Mean-Field Approximation. To sum up all orders in $-1/t$, we apply the mean-field method, which works very well for the static potential (for a review, see [1]).

The (variational) mean-field ansatz with fluctuations included reads

$$X^\mu(x,y) = \frac{1}{\pi K}\sum_i p_i^\mu \arctan\frac{(x-s_i)}{y} + X_{\rm q}^\mu(x,y). \tag{55}$$

The momenta p_i's and, correspondingly, the Mandelstam variables s and t are fixed, while the ratio r (defined in Eq. (48)) is a variational parameter:

$$S_{\rm mf} = \alpha' s \ln r + \alpha' t \ln(1-r) + \frac{(d-2)}{24}\ln(1-r) \quad \text{valid as } r \to 1. \tag{56}$$

The first two terms on the right-hand side result from the classical quadratic action (in the conformal gauge), while the third term is the momentum Lüscher term computed by Janik [23], Makeenko [7].

Minimizing with respect to r, we find

$$r_* = 1 - \frac{\alpha' t + (d-2)/24}{\alpha' s} \tag{57}$$

which results in the linear Regge trajectory

$$\alpha(t) = \frac{(d-2)}{24} + \alpha' t, \tag{58}$$

coinciding with the semiclassical one (51).

The mean field usually works at large d, but is expected to be exact for bosonic string at any d. The arguments are given in [8]. Quadratic fluctuations about this mean field are stable for $\alpha(t) < 0$, that is $-\alpha' t > (d-2)/24$. We can go beyond this domain by an analytic continuation.

3. FROM BOSONIC STRING TO QCD

3.1. Consistent Off-Shell Amplitudes. We have already seen in Subsec. 2.3 that off-shell scattering amplitudes involve the reparameterization path integral. Choosing the Lovelace choice (25) of the discretization of the measure and of the Green function at coinciding arguments:

$$\mathcal{D}^{(N)}_{\text{diff}} s = \prod_{i=1}^{N} \frac{ds_i\,(s_{i+1} - s_{i-1})}{(s_{i+1} - s_i)(s_i - s_{i-1})} \tag{59}$$

and

$$G\,(s_j, s_j) \overset{\text{Lovelace}}{=} \frac{1}{\pi} \ln \frac{(s_{j+1} - s_{j-1})}{(s_{j+1} - s_j)(s_j - s_{j-1})\varepsilon}\,, \tag{60}$$

it is possible to integrate over s_i's at the intermediate points, at which $p^\mu(t)$ has no discontinuities.

As is shown by Makeenko, Olesen [6], this results in the scattering amplitude

$$A(p_1, \ldots, p_M) = \\ = \int\limits_{s_{i-1} < s_i} \prod_{i=1}^{M} ds_i \prod_{k \neq l}^{M} |s_k - s_l|^{\alpha' p_k \cdot p_l} \prod_{j=1}^{M} \left(\frac{|s_j - s_{j-1}|\,|s_{j+1} - s_j|}{|s_{j+1} - s_{j-1}|} \right)^{\alpha' p_j^2 - 1}. \tag{61}$$

The remaining integration over s_i's (the Koba–Nielsen variables), at which $p^\mu(t)$ has discontinuities, is inherited from the path integral over reparameterizations.

Remarkably, the off-shell amplitude (61) is a consistent off-shell projective-invariant tree string amplitude known from [25]. It is invariant under $PSL(2;\mathbb{R})$ for arbitrary p_i^2. For the tachyonic case, when all $p_i^2 = 1/\alpha'$, the last factor on the right-hand side of Eq. (61) equals 1 and the amplitude (61) reproduces the Koba–Nielsen one.

3.2. Application to QCD. Meson scattering amplitudes in QCD can be extracted from Green's functions of M colorless composite quark operators of the type

$$\bar{q}(x_i)q(x_i), \quad \bar{q}(x_i)\gamma_5 q(x_i), \quad \bar{q}(x_i)\gamma_\mu q(x_i), \quad \bar{q}(x_i)\gamma_\mu\gamma_5 q(x_i), \quad \text{etc.} \tag{62}$$

These Green functions are given by the sum over Wilson loops, passing via the points x_i $(i = 1, \ldots, M)$ at which the operators are inserted:

$$G \equiv \left\langle \prod_{i=1}^{M} \bar{q}(x_i)q(x_i) \right\rangle_{\text{conn}} \overset{\text{large } N}{=} \sum_{\text{paths} \ni \{x_1, \ldots, x_M \equiv x_0\}} J[x(\tau)]\, W[x(\tau)]. \tag{63}$$

Here the Wilson loop $W[x(\tau)]$ is in pure Yang–Mills at the large number of colors N (or quenched). This important observation by Makeenko, Migdal [26] is a consequence of the large-N factorization. The correlators of several Wilson loops are present at finite N.

There exist many ways of representing the weight for the path integration in the worldline formalism. I shall use a momentum-space disentangling of gamma matrices, where

$$J[x(\tau)] = \int \mathcal{D}k(\tau)\ \mathrm{sp}\ \boldsymbol{P} \exp\left\{ i \int\limits_0^{\mathcal{T}} d\tau\, [\dot{x}(\tau)\cdot k(\tau) - \gamma \cdot k(\tau)] \right\} \tag{64}$$

for spinor quarks and scalar operators. Here τ is the proper time and sp is the trace of the path-ordered product of gamma matrices. This representation is most convenient for dealing with the momentum loops as we shall shortly see.

Doing the functional Fourier transformation (28), we obtain, as shown by Makeenko, Olesen [2], the following representation for the meson scattering amplitude:

$$A\,(p_1,\ldots,p_M) = \sum_{\mathrm{paths}} \exp\left[i \int\limits_0^{\mathcal{T}} d\tau\, \dot{x}(\tau)\cdot p(\tau) \right] J[x(\tau)]\, W[x(\tau)], \tag{65}$$

where $p^\mu(\tau)$ is the piecewise constant momentum loop (29).

Substituting for $W[x(\tau)]$ the reparameterization path integral (1) and interchanging the integrals over $x(\tau)$ (Gaussian) and $s(\tau)$, we find

$$A\,(p_1,\ldots,p_M) \propto \int\limits_0^\infty d\mathcal{T}\, \mathcal{T}^{M-1}\, \mathrm{e}^{-m\mathcal{T}} \int\limits_{-\infty}^{+\infty} \frac{ds_{M-1}}{1+s_{M-1}^2} \prod_{i=1}^{M-2} \int\limits_{-\infty}^{s_{i+1}} \frac{ds_i}{1+s_i^2} \times$$
$$\times \int \mathcal{D}k(t)\ \mathrm{sp}\ P \exp\left[-i\mathcal{T} \int dt \frac{\gamma\cdot k(t)}{1+t^2} \right] W\Big[x(t) = \frac{1}{K}\,(p(t)+k(t)) \Big]. \tag{66}$$

It looks like the stringy amplitude (32), but with an additional path integral over $k^\mu(\tau)$.

The latter path integral over $k^\mu(\tau)$ remarkably factorizes for small quark mass m^* and/or large M since the integral over $\mathcal{T}$ is dominated by large $\mathcal{T} \sim (M-1)/m$ and typical $k \sim 1/\mathcal{T}$. We thus obtain just the same Lovelace-type string amplitude

$$A\,(p_1,\ldots,p_M) \propto W\Big[x(t) = \frac{1}{K} p(t) \Big] \tag{67}$$

as discussed in the previous subsection.

This result, however, cannot be exact for QCD string since the reparameterization path integral (1) applies only for large loops. Perturbative QCD applies instead for small loops. Nevertheless, large loops dominate the path integral over $x^\mu(\tau)$ in Eq. (28) in the Regge kinematical regime, as is shown by Makeenko,

*A similar observation was first made by Janik, Peschanski [27] (see also [28]), using a different representation of the spinor weight.

Olesen [9]. This is a pure stringy phenomenon that large momenta are associated with large distances. In perturbation theory there is no dimensional parameter like the string tension and large momenta are associated with small distances.

3.3. Effective ρ-Trajectory and pQCD Prediction. The above results on the linear Reggeon trajectory in large-N QCD can be compared with experiment. We should bear in mind that the string disc amplitude is associated with planar graphs and therefore with the ρ-meson type Regge trajectories. It is to be distinguished from the Pomeron trajectory, which is associated with cylinder graphs.

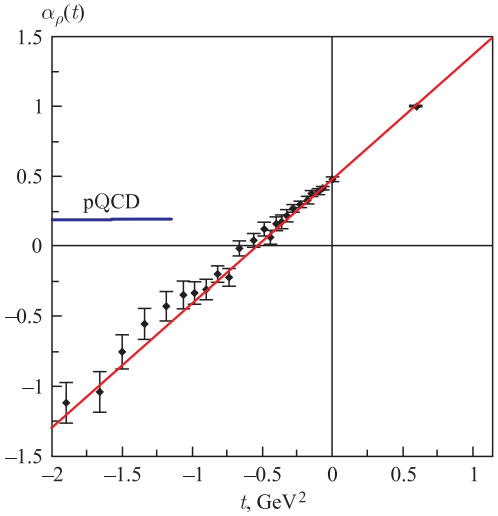

Fig. 5. Effective ρ-meson trajectory extracted from the exclusive process $\pi^- p \to \pi^0 n$. The figure taken from [29]

The effective ρ-meson trajectory, extracted from the exclusive process $\pi^- p \to \pi^0 n$, is reproduced in Fig. 5. The figure is taken from [29]. It is seen in the figure that the linear trajectory of the intercept ≈ 0.5, known from the spectrum for positive t, continues to negative t down to $t \approx -2$ GeV^2. The (almost horizontal) line to the left in Fig. 5 corresponds to perturbative QCD reggeization of $\bar{q}q$ by Kirschner, Lipatov [30], which is expected to work for $t \lesssim -$few GeV^2. As we argue in the next subsection, such a behavior of the experimental results is because the value of s was not large enough.

3.4. Separation of pQCD and QCD String. Let us consider a very simple model of QCD string, when the Wilson loop equals 1 for $KS_{\min} < 1$ and is given by Eq. (1) for $KS_{\min} > 1$. We have thus disregarded gluon interactions and restricted ourselves with the free contribution for small loops. The motivation is that the interaction is then small (owing to asymptotic freedom) and the quark counting rule (the Bjorken scaling) applies for large $-t$, resulting in the Reggeon

trajectory $\alpha(t) = 0$. For large loops, we substitute a dual description by the string disk amplitude (1). An analogy with the AdS/CFT correspondence is as if we were to substitute either the Wilson loop in $\mathcal{N} = 4$ super Yang–Mills at small values of the coupling constant or IIB open superstring in $AdS_5 \times S^5$ at large couplings.

We can yet simplify the model, separating large and small loops by the value of their length rather than the minimal area. This is legitimate because QCD string is smooth (not crumpled) so the typical values of the minimal area are proportional to the length squared, $S_{\min} \propto L^2$. We thus substitute

$$W(C) = \begin{cases} 1 & \text{for } \sqrt{K}L < 1, \\ \text{Eq. (1)} & \text{for } \sqrt{K}L > 1. \end{cases} \tag{68}$$

In practice this means that when the proper time $\mathcal{T}$ is smaller than $\tau_{\max} \sim 1/K$, we pick up the contribution from small loops and when it is larger than $\tau_{\max} \sim 1/K$, we pick up the contribution from large loops. Thus $\tau_{\max} \sim 1/K$ plays the role of an infrared cutoff in perturbative QCD instead of the usual transverse mass μ.

A nice feature of the ansatz (68) is that the meson scattering amplitude (65) can now be straightforwardly computed and equals the sum of the contribution of perturbative QCD and QCD string with a certain relative coefficient, which is of most importance at finite s. It is the only parameter to be fixed below by comparing with experimental data. At infinite s, there remains the contribution from either perturbative QCD or QCD string, depending on whose exponent is larger at given t. However, at finite s, both contributions are essential and the lower s is the more essential the QCD string contribution becomes at $-t \approx$ few GeV^2.

In Fig. 6, we compare the experimental data by Kennett et al. [31] for the ρ-meson trajectory, extracted from the inclusive process $\pi^- p \to \pi^0 x^0$, with the prediction of the model (68). The relative coefficient is fixed to fit the data at $s = 400$ GeV^2 (the lower line in the bottom figure). The upper the line is the larger s is. As $s \to \infty$, the two regimes separate. The model we have considered quantifies the idea of Brodsky, Tang, Thorn [32] about the mixing of the two regimes in QCD at finite s.

4. CONCLUSION AND OUTLOOK

The Regge behavior of meson scattering amplitudes can be derived for QCD string under practically the only assumption that N is large. Great simplifications occur for small quark mass and/or large number of colliding mesons.

It was crucial for the success of calculations that all integrals are Gaussian except for the one over reparameterizations which reduces to the integration over the Koba–Nielsen variables.

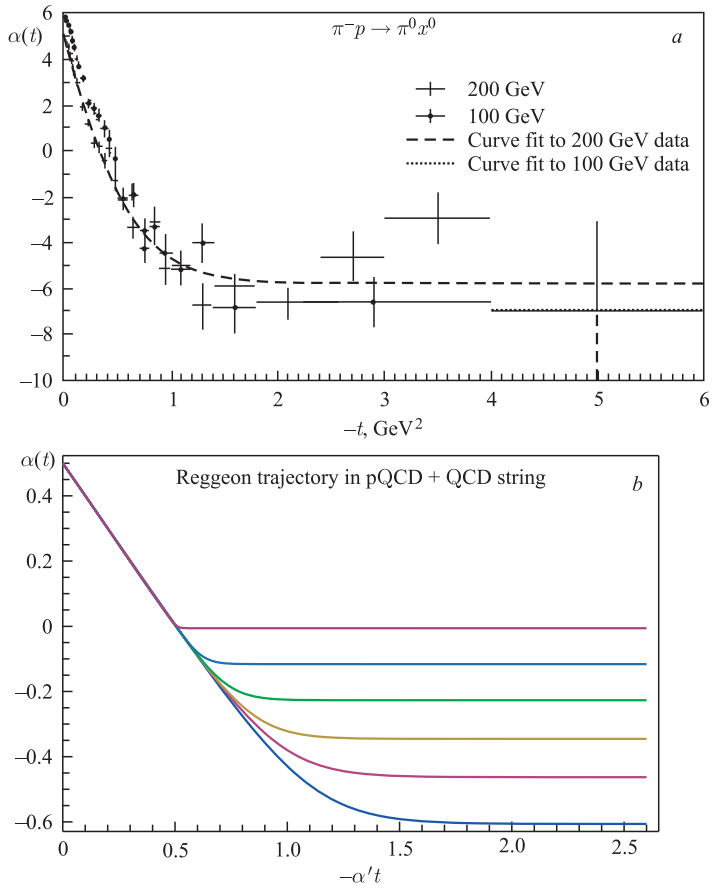

Fig. 6. Experimental data by Kennett et al. [31] (*a*) and their description by pQCD + QCD string (*b*). The smaller the value of s the lower is the line

The mean-field approximation results for QCD string in the linear Reggeon trajectory of the intercept $\alpha(0) = (d-2)/24$. The actual Reggeon intercept of $\alpha(0) \approx 0.5$ has to be obtained, most probably, by accounting for spontaneous breaking of chiral symmetry.

When $-t \ll s$ becomes large, there are no longer reasons to expect the contribution of QCD string to dominate over perturbation theory. The relative contribution of the two changes with increasing s.*

*It would be most interesting to extend this kind of consideration to the singlet channel, where the next order of pQCD is known for the BFKL (Balitsky–Fadin–Kuraev–Lipatov) pomeron.

At the end I shall mention some existing extensions of Douglas' boundary functional and the reparameterization path integral to

— closed string (with a possible application to gravity) by Caputa, Hirano [33],

— the RNS (Ramond–Neveu–Schwarz) superstring by Caputa [34],

— the GS (Green–Schwarz) superstring in the $AdS_5 \times S^5$ background (dual to $\mathcal{N} = 4$ super Yang–Mills) by Ambjørn, Makeenko [35] and Kristjansen, Makeenko [36].

REFERENCES

1. *Makeenko Y.* QCD String as an Effective String. arXiv:1206.0922[hep-th].
2. *Makeenko Y., Olesen P.* Implementation of the Duality between Wilson Loops and Scattering Amplitudes in QCD // Phys. Rev. Lett. 2009. V. 102. P. 071602; arXiv:0810.4778 [hep-th].
3. *Makeenko Y., Olesen P.* Wilson Loops and QCD/String Scattering Amplitudes // Phys. Rev. D. 2009. V. 80. P. 026002; arXiv:0903.4114[hep-th].
4. *Buividovich P., Makeenko Y.* Path Integral over Reparameterizations: Levy Flights versus Random Walks // Nucl. Phys. B. 2010. V. 834. P. 453; arXiv:0911.1083[hep-th].
5. *Makeenko Y., Olesen P.* Quantum Corrections from a Path Integral over Reparameterizations // Phys. Rev. D. 2010. V. 82. P. 045025; arXiv:1002.0055[hep-th].
6. *Makeenko Y., Olesen P.* Semiclassical Regge Trajectories of Noncritical String and Large-N QCD // JHEP. 2010. V. 1008. P. 095; arXiv:1006.0078[hep-th].
7. *Makeenko Y.* Effective String Theory and QCD Scattering Amplitudes // Phys. Rev. D. 2011. V. 83. P. 026007; arXiv:1012.0708[hep-th].
8. *Makeenko Y.* An Interplay between Static Potential and Reggeon Trajectory for QCD String // Phys. Lett. B. 2011. V. 699. P. 199; arXiv:1103.2269[hep-th].
9. *Makeenko Y., Olesen P.* The QCD Scattering Amplitude from Area Behaved Wilson Loops // Phys. Lett. B. 2012. V. 709. P. 285; arXiv:1111.5606[hep-th].
10. *Polyakov A. M.* Talk at the Workshop «Particles, Fields and Strings», Vancouver, 1997. Unpublished.
11. *Polyakov A. M.* Quantum Geometry of Bosonic Strings // Phys. Lett. B. 1981. V. 103. P. 207; Gauge Fields and Strings. Harwood Acad. Publ., 1987.
12. *Alvarez O.* Theory of Strings with Boundaries: Fluctuations, Topology and Quantum Geometry // Nucl. Phys. B. 1983. V. 216. P. 125.
13. *Cohen A. G. et al.* An Off-Shell Propagator for String Theory // Nucl. Phys. B. 1986. V. 267. P. 143.
14. *Douglas J.* Solution of the Problem of Plateau // Trans. Am. Math. Soc. 1931. V. 33. P. 263.
15. *Polchinski J., Strominger A.* Effective String Theory // Phys. Rev. Lett. 1991. V. 67. P. 1681.

16. *Horowitz J.* The Hausdorff Dimension of the Sample Path of a Subordinator // Israel J. Math. 1968. V. 6. P. 176.
17. *Migdal A. A.* Momentum Loop Dynamics and Random Surfaces in QCD // Nucl. Phys. B. 1986. V. 265. P. 594.
18. *Alday L. F., Maldacena J.* Gluon Scattering Amplitudes at Strong Coupling // JHEP. 2007. V. 0706. P. 064; arXiv:0705.0303[hep-th].
19. *Drummond J. M., Korchemsky G. P., Sokatchev E.* Conformal Properties of Four-Gluon Planar Amplitudes and Wilson Loops // Nucl. Phys. B. 2008. V. 795. P. 385; arXiv:0707.0243[hep-th].
20. *Brandhuber A., Heslop P., Travaglini G.* MHV Amplitudes in $N = 4$ Super-Yang–Mills and Wilson Loops // Nucl. Phys. B. 2008. V. 794. P. 231; arXiv:0707.1153[hep-th].
21. *Aoyama H., Dhar A., Namazie M. A.* Covariant Amplitudes in Polyakov's String Theory // Nucl. Phys. B. 1986. V. 267. P. 605.
22. *Hsue C. S., Sakita B., Virasoro M. A.* Formulation of Dual Theory in Terms of Functional Integrations // Phys. Rev. D. 1970. V. 2. P. 2857.
23. *Janik R. A.* String Fluctuations, AdS/CFT and the Soft Pomeron Intercept // Phys. Lett. B. 2001. V. 500. P. 118; arXiv:hep-th/0010069.
24. *Durhuus B., Olesen P., Petersen J. L.* On the Static Potential in Polyakov's Theory of the Quantized String // Nucl. Phys. B. 1984. V. 232. P. 291.
25. *Di Vecchia P. et al.* N-String Vertex and Loop Calculation in the Bosonic String // Nucl. Phys. B. 1988. V. 298. P. 526.
26. *Makeenko Y. M., Migdal A. A.* Quantum Chromodynamics as Dynamics of Loops // Nucl. Phys. B. 1981. V. 188. P. 269.
27. *Janik R. A., Peschanski R.* Reggeon Exchange from AdS/CFT // Nucl. Phys. B. 2002. V. 625. P. 279; arXiv:hep-th/0110024.
28. *Giordano M., Peschanski R.* Reggeon Exchange from Gauge/Gravity Duality // JHEP. 2011. V. 1110. P. 108; arXiv:1105.6013[hep-th].
29. *Kaidalov A. B.* Some Problems of Diffraction at High Energies. arXiv:hep-th/0612358.
30. *Kirschner R., Lipatov L. N.* Double Logarithmic Asymptotics and Regge Singularities of Quark Amplitudes with Flavor Exchange // Nucl. Phys. B. 1983. V. 213. P. 122.
31. *Kennett R. G. et al.* The Production of Neutral Pions from 200-GeV $\pi^- p$ Collisions in the High x Region // Nucl. Phys. B. 1987. V. 284. P. 653.
32. *Brodsky S. J., Tang W. K., Thorn C. B.* The Reggeon Trajectory in Exclusive and Inclusive Large Momentum Transfer Reactions // Phys. Lett. B. 1993. V. 318. P. 203.
33. *Caputa P., Hirano S.* Observations on Open and Closed String Scattering Amplitudes at High Energies // JHEP. 2012. V. 1202. P. 111; arXiv:1108.2381[hep-th].
34. *Caputa P.* Lightlike Contours with Fermions // Phys. Lett. B. 2012. V. 716. P. 475; arXiv:1205.6369[hep-th].
35. *Ambjørn J., Makeenko Y.* Remarks on Holographic Wilson Loops and the Schwinger Effect // Phys. Rev. D. 2012. V. 85. P. 061901; arXiv:1112.5606[hep-th].
36. *Kristjansen C., Makeenko Y.* More about One-Loop Effective Action of Open Superstring in $AdS_5 \times S^5$ // JHEP. 2012. V. 1209. P. 053; arXiv:1206.5660[hep-th].